PROCEEDINGS OF SPIE

SPIEDigitalLibrary.org/conference-proceedings-of-spie

Quantitative dynamic MRI (QdMRI) volumetric analysis of pediatric patients with thoracic insufficiency syndrome

Yubing Tong, Jayaram K. Udupa, E. Paul Wileyto, Caiyun Wu, Joseph M. McDonough, et al.

Yubing Tong, Jayaram K. Udupa, E. Paul Wileyto, Caiyun Wu, Joseph M. McDonough, Anthony Capraro, Oscar H. Mayer, Drew A. Torigian, Robert M. Campbell, "Quantitative dynamic MRI (QdMRI) volumetric analysis of pediatric patients with thoracic insufficiency syndrome," Proc. SPIE 10578, Medical Imaging 2018: Biomedical Applications in Molecular, Structural, and Functional Imaging, 1057806 (12 March 2018); doi: 10.1117/12.2294048

SPIE.

Event: SPIE Medical Imaging, 2018, Houston, Texas, United States

Quantitative dynamic MRI (QdMRI) Volumetric Analysis of Pediatric Patients with Thoracic Insufficiency Syndrome

Yubing Tong[1], Jayaram K. Udupa[1*], E. Paul Wileyto[3], Caiyun Wu[1],

Joseph M. McDonough[2], Anthony Capraro[2], Oscar H. Mayer[2], Drew A. Torigian[1], Robert M. Campbell Jr.[2]

[1]Medical Image Processing Group, Department of Radiology, University of Pennsylvania, Philadelphia, PA, 19104 , United States; [2]Center for Thoracic Insufficiency Syndrome, Children's Hospital of Philadelphia, Philadelphia, PA, 19104, United States; [3]Data Management and Biostatistics Core for the Tobacco Use Research Center, University of Pennsylvania, Philadelphia, PA, 19104 , United States.

ABSTRACT

The lack of standardizable objective diagnostic measurement techniques is a major hurdle in the assessment and treatment of pediatric patients with thoracic insufficiency syndrome (TIS). The aim of this paper is to explore quantitative dynamic MRI (QdMRI) volumetric parameters derived from thoracic dMRI in pediatric patients with TIS and the relationships between dMRI parameters and clinical measurements. 25 TIS patients treated with vertical expandable prosthetic titanium rib (VEPTR) surgery are included in this retrospective study. Left and right lungs at end-inspiration and end-expiration are segmented from constructed 4D dMRI images. Lung volumes and excursion (or tidal) volumes of the left/right chest wall and hemi-diaphragms are computed. Commonly used clinical parameters include thoracic and lumbar Cobb angles and respiratory measurements from pulmonary function testing (PFT). 200 3D lungs in total (left & right, pre-operative & post-operative, end-inspiration & end-expiration) are segmented for analysis. Our analysis indicates that change of resting breathing rate (RR) following surgery is negatively correlated with that of QdMRI parameters. Chest wall tidal volumes and hemi-diaphragm tidal volumes increase significantly following surgery. Clinical parameter RR reduced after surgical treatment with P values around 0.06 but no significant differences were found on other clinical parameters. The significant increase in post-operative tidal volumes suggests a treatment-related improvement in lung capacity. The reduction of RR following surgery shows that breathing function is improved. The QdMRI parameters may offer an objective marker set for studying TIS, which is currently lacking.

Keywords: Quantitative dynamic MRI (QdMRI), lung, tidal volume, thoracic insufficiency syndrome (TIS), pediatric thoracic function.

1. INTRODUCTION

Thoracic insufficiency syndrome (TIS) is known to be associated with at least 28 pediatric diseases, often due to a thoracic volume depletion deformity, and TIS patients usually have the inability of the thorax to support normal respiration or lung growth [1]. Younger patients with severe spine and chest wall malformations can be treated with FDA-approved growth-sparing thoracic expansion devices known as vertical expandable prosthetic titanium rib (VEPTR), with the assumption that the enlarged chest cavity will trigger lung growth by the stretch reflex and the larger lungs will be powered in respiration primarily by the diaphragm [2, 3]. The major hurdles currently preventing advancement and innovation in TIS assessment and treatment include the lack of standardizable objective diagnostic measurement techniques that describe the 3D thoraco-abdominal structures, the dynamics of respiration, and the changes that take place with growth. Dynamic computed tomography (CT) [4-6] can define thoracic function, but poses serious

Medical Imaging 2018: Biomedical Applications in Molecular, Structural, and Functional Imaging, edited by Barjor Gimi, Andrzej Krol, Proc. of SPIE Vol. 10578, 1057806 · © 2018 SPIE
CCC code: 1605-7422/18/$18 · doi: 10.1117/12.2294048

concerns of radiation exposure in pediatric population. Dynamic magnetic resonance imaging (dMRI) [7-9] is a radiation-free image acquisition technique which allows for natural free breath-

ing, without requiring breath-holding or wearing of devices for acquiring gating signals, and is the most suitable imaging modality for TIS patients because of the often-present severe thoracic deformation. Previous reports of older patients with dMRI [10] used breath-hold techniques. Current approaches for surgical planning include radiographs and CT scans to determine thoracic deformity/constriction in order to select the best surgery to straighten the spine and equilibrate the thorax, but dynamic abnormalities seen on dMRI may alter these strategies. In the current study, dMRI scans are acquired during tidal breathing. The aim of this paper is to explore quantitative dynamic MRI (QdMRI) volumetric parameters derived from thoracic dMRI in pediatric patients with TIS and the relationships between dMRI parameters and clinical measurements.

In this study, dMRI images are acquired for the first time from a true tidal breathing way. We report the quantitative volumetric parameters derived from dynamic MRI before and after VEPTR surgery (Pre-/Post-op). We also compare these parameters with those from pulmonary function tests to understand the effectiveness of surgery. The methods have the potential to provide a new metric for determining the effectiveness of pediatric spine and chest wall devices in restoring thoracic function for respiration. To our knowledge, such full 4D dynamic analysis techniques to investigate how the derived parameters may be useful to objectively study TIS patient conditions and their treatment outcome have not been previously attempted.

2. MATERIALS AND METHODS

Subjects

This retrospective study was conducted following approval from the Institutional Review Board at the Children's Hospital of Philadelphia along with a Health Insurance Portability and Accountability Act waiver. Reconstructed 4D MR images of 25 pediatric TIS patients (12 male, 13 female) with age 5.10 ± 4.21 years (pre-operatively) and 6.72 ± 4.21 years (post-operatively after placement of VEPTR) are considered in this investigation. 4D dMRI images of those subjects include 4-8 time points during one breathing cycle with voxel size 1.17×1.17×6.0 mm^3 and 3D scene size of 224×256×30-40. In this study, we mainly focus on left/right lung volumes and excursion (or tidal) volumes derived from dMRI at end-inspiration and end-expiration.

Dynamic MR image acquisition and 4D image construction

In this study, 4D images from the acquired dMRI scans are constructed by utilizing the recently developed approach of 4D dMRI image construction [11] from free-breathing MRI slice acquisitions. Acquisition parameters: TrueFISP with TR/TE ~ 4.3/2.2 msec, 1.5 Tesla scanner [11]. For each subject, at each sagittal slice location named as z-position, 80-100 slices are acquired at ~200 msec/slice over several tidal breathing cycles, where each slice has a corresponding phase location in one breathing cycle named as t-position. Going through all t- and z- positions, this produces thousands (2500~3000) of slices per patient, which represent an unordered sampling of the 4D free-breathing patient thorax over multiple breathing cycles. A graph-based optimization approach was developed for constructing the best possible 4D volume from such data [11]. The approach first builds a graph in which each node represents an acquired 2D slice with a specific z and t value. Weights are assigned to the arcs between any two nodes at neighboring location based on the measure of temporal and spatial contiguity of slices. From every node corresponding to the first z location, an optimal path (with smallest total cost) is found to some node in the last z location. The slices representing the nodes in this path constitute an optimal 3D volume for one time instance. Subsequently, from all such optimal volumes found for all t-positions, the best respiratory period comprising a 4D volume is found. Usually 200~300 slices in total across all

locations are selected among 2500~3000 acquired free breathing slices to construct one 4D image over one breathing cycle. The method guarantees a globally optimal solution and does not need any external instruments to record respiratory motion/signal or tidal volume.

Image processing and segmentation

4D dMRI images are processed to improve signal quality and consistency by using non-uniformity correction and intensity standardization techniques [12, 13]. Non-uniformity correction improves the homogeneity of the same tissue, and intensity standardization makes the intensity of each tissue (for all patients, pre-operatively and post-operatively) to have the same numeric meaning. Interactive iterative relative fuzzy connectedness (*i*-IRFC) is used as the engine for lung segmentation [14]. With *i*-IRFC, the users can easily control the final segmentation and make sure that "what you see is what you get".

Image-derived markers and clinical measurements

From separate segmentations of the left and right lungs at end-inspiration and end-expiration, by subtracting segmentations, and performing morphological operations and connected component labeling, we obtain 11 key volume parameters in total from each 4D dMRI data set including 7 parameters for tidal volumes and 4 for lung volumes. We refer to the change in volume of a structure from end-inspiration to end-expiration as tidal volume (tv). The 7 tidal volume parameters thus obtained are: lung TV (Ltv), left lung TV (LLtv), right lung TV (RLtv), left chest wall TV (LCWtv), right chest wall TV (RCWtv), left hemi-diaphragm TV (LDtv), and right hemi-diaphragm TV (RDtv). The 4 lung volume parameters are left and right lung volume at end-inspiration (L/R LVei) and left and right lung volume at end-expiration (L/R LVee).

Table 1. QdMRI parameters and clinical measurements.

		Parameters	Description
QdMRI parameters		LLVei, RLVei	left and right lung volume at end-inspiration
		LLVee, RLVee	left and right lung volume at end-expiration
		L/R CWtv	left/right chest wall tidal volumes
		L/R Dtv	left/right hemi-diaphragm tidal volumes
		L/R Ltv	left/right lung tidal volumes
		Ltv	lung tidal volumes = L Lev + R Ltv
Clinical parameters	PFT	FVC	forced vital capacity
		TLC	total lung capacity
	Other	RR	resting breathing rate
		AVR	assisted ventilation rating
		L/R ALS	left/right available lung space
	Cobb Angles	Signed TCA/LCA	Thoracic and lumbar Cobb angle from AP radiograph; Positive means spine convexity to the right, and Negative means spine convexity to the left

As commonly used, clinical measurements include: forced vital capacity (FVC) and total lung capacity (TLC) from pulmonary function testing (PFT) [15], Cobb angle of spinal curves from AP radiographs, and other parameters of resting breathing rate (RR); assisted ventilation rating (AVR), and left/right available lung space (ALS). Table 1 lists all parameters utilized for analysis in this study.

3. RESULTS

Figure 1 shows pre-operative and post-operative rendered lung images of a patient where the thoracolumbar spinal curvature is observed preoperatively and no curvature is seen postoperatively. The figure shows 3D MRI lung surface renditions at end-inspiration and end-expiration before and after surgery. Notice how the lung volumes have significantly enlarged post-operatively (displays are portrayed proportionately to scale).

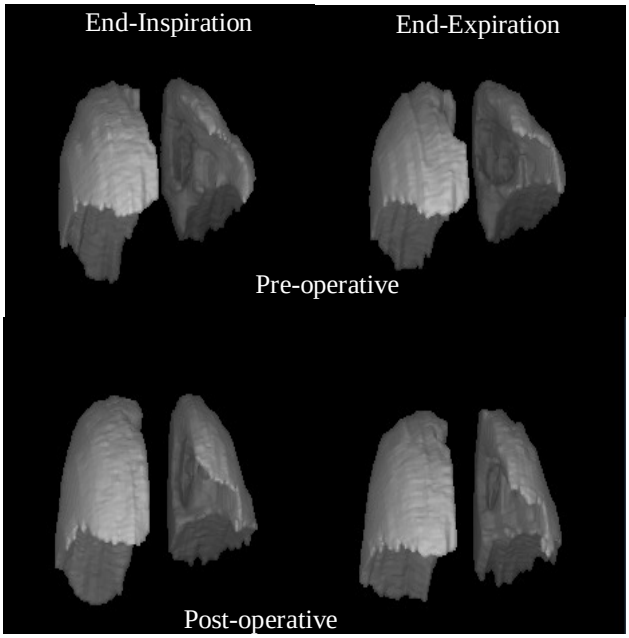

Figure 1. 3D renditions of the lungs of an 11-year old male TIS patient with neuromuscular scoliosis are shown. 1st row: Pre-op images. 2nd row: Post-op images. Lungs at end-inspiration and end-expiration are displayed in the 2nd and 3rd columns, respectively.

Table 2. Key QdMRI parameters (in cc) and Cobb angles (degree) before and after surgery.

Volume in cc		LCWtv	RCWtv	LDtv	RDtv	LLVee	LLVei	RLVee	RLVei	TCA	LCA
Pre-operative	Mean	21.397	28.120	11.428	21.596	199.677	299.010	205.911	316.540	55.5	26.4
	SD	11.373	14.565	6.198	12.389	154.687	260.653	158.998	263.846	31.7	41.9
Post-operative	Mean	28.558	38.430	18.448	37.169	223.577	343.942	252.660	399.534	44.2	21.5
	SD	13.318	15.352	11.731	20.073	133.998	222.445	150.326	243.443	28.0	31.0

Table 2 lists the key QdMRI volumetric parameters and Cobb angles to describe the spinal curves for all 25 patients pre-operatively and post-operatively with mean and standard deviation (SD) values reported. The table also shows lung volumes at end-inspiration (EI) and end-expiration (EE) in addition to the tidal volumes. These are denoted: LLVei, LLVee, RLVei, and RLVee.

All dMRI volumes increase from pre-operative to post-operative condition, with an average increase of 21.6% for mean volume and 50.7% for median volume. Both TCA and LCA decreased from pre-operative to post-operative condition with a reduction of 20.3% for mean Cobb angle and 18.6% for median Cobb angle, which means that the thoracolumbar spine has less scoliotic curvature on the AP radiograph after surgical treatment.

Table 3. Statistical analysis of dMRI excursion volumes with Cobb angle measurements, AVR, and FVC.

	Coef.	Standard Error	z score	p value	effect size
LDtv vs. LCA	0.137	0.046	2.958	0.003	0.892
RDtv vs. LCA	-0.122	0.066	-1.860	0.063	0.561
LDtv vs. TCA	-0.078	0.044	-1.792	0.073	0.422
RDtv vs. TCA	-0.089	0.042	-2.116	0.034	0.499
LDtv vs. max (LCA, TCA)	0.109	0.058	1.860	0.063	0.438

Table 3 explores the association of QdMRI parameters with clinical variables, specifically Cobb angles. Other types of analyses with other clinical parameters are currently being carried out.

All tidal volumes showed large positive changes from pre- to post-op condition. The values were correlated within subject (average correlation 0.63). Since the patients may have grown from pre- to post-op, we adjusted for predicted tidal volume using known data for matched normal subjects [17]. Our model indicated significant pre- to post-op change that could only be explained by the surgery. Data for left & right chest wall and diaphragmatic components of tidal volume are shown in Table 3. Cobb angle did not predict any of the tidal volumes. Other clinical variable were variable in their ability to predict dMRI tidal volumes (data not shown here).

RR was unrelated to tidal volumes. Effect sizes for the clinical variables were large. In words, the changes in chest wall and diaphragmatic tidal volumes from pre- to post-op condition were positive and large indicating significant gain in the chest wall and diaphragmatic components of lung function post-operatively.

4. CONCLUSIONS

The thorax is a complex respiratory engine with the chest wall, rib cage, spine, and diaphragm as its deformable and/or dynamic components. Although PFT is employed to infer thoracic function, it gives a global indication of function and cannot resolve the dynamics or the role of substructures in the overall function. In TIS and other ailments associated with thoracic deformities, the deficits are rarely symmetric, and hence global and integrative measures like those derived from PFT are useful for an overall understanding of the ailment and its treatment outcomes, but not for close scrutiny of the unilateral roles of substructures or their changes due to treatment. The proposed method is the only approach to obtain detailed information about structures and their dynamics for understanding and examining closely the effect of surgery on thoracic components and function.

In this study, we explored quantitative dynamic MRI (QdMRI) volumetric parameters derived from thoracic dMRI in pediatric patients with TIS as well as the relationships between dMRI parameters and clinical measurements of Cobb angle and PFT. We also proposed a complete stream-lined approach of analysis to provide objective dynamic functional metrics to understand current TIS surgical methods and facilitate innovation of new procedures. Although the analysis is currently done on the end-inspiration and end-expiration time points, more 3D volumes at different time points can be used in future to better understand the breathing motion in 4D space for TIS patients. Dynamic lung MRI has great potential to clearly define quantitatively, without radiation concerns, the dynamic biomechanical deficits and the response to treatment of the dynamic thoraco-abdominal organs of young patients with TIS. The QdMRI approach may fill this void that currently exists in this field.

Acknowledgement

The research reported here is funded by a DHHS grant R21 HL124462 and a "Frontier" grant from the Children's Hospital of Philadelphia.

References

[1] Campbell, RM Jr. and Smith, MD: "Thoracic insufficiency syndrome and exotic scoliosis," The Journal of Bone and Joint Surgery, 89A (Supplement 1):108-122, 2007.
[2] Campbell RM Jr, Smith MD: "Reconstruction of the thorax in patients with absent ribs and flail chest physiology using vertical expandable prosthetic titanium ribs (VEPTR)," Presented as a poster exhibit at the Annual Meeting of the American Pediatric Surgical Association, May 24-28, Fort Lauderdale, FL, 2003.
[3] Campbell RM Jr, Smith MD, Hell-Vocke AK: "Expansion thoracoplasty: the surgical technique of open-wedge thoracostomy [surgical technique]," J Bone Joint Surg Am., 86:S51-S64, 2004.
[4] Nehmeh SA, Erdi YE, Pan T, Pevsner A, Rosenzweig KE, Yorke E, Mageras GS, Schoder H, Vernon P, Squire O, Mostafavi H, Larson SM, Humm JL.: "Four-dimensional (4D) PET/CT imaging of the thorax," *Medical Physics*, 31(12):3179-3186, 2004.
[5] Keall, PJ, Vedam, SS, George, R.: "Technical Report, Respiratory regularity gated 4D CT acquisition: concepts and proof of principle," *Australas Phys Eng Sci Med*., 30(3):211-220, 2007.
[6] Low DA, Nystrom M, Kalinin E, Parikh P, Dempsey JF, Bradley JD, Islam T, Christensen G, Politte DG, Whiting BR.: "A method for the reconstruction of four-dimensional synchronized CT scans acquired during free breathing," *Medical Physics*, 30(6):1254-1263, 2003.
[7] Wachinger C, Yigitsoy M, Rijkhorst EJ, Navab N.: "Manifold learning for image-based breathing gating in ultrasound and MRI," *Med Image Anal*., 16(4):806-818, 2012.
[8] Cai J, Chang Z, Wang Z, Paul Segars W, Yin FF.: "Four-dimensional magnetic resonance imaging (4D-MRI) using image-based respiratory surrogate: a feasibility study," *Medical Physics*, 38(12):6384-6394, 2011.
[9] Wagshul ME, Sin S, Lipton ML, Shifteh K, Arens R.: "Novel retrospective, respiratory-gating method enables 3D, high resolution, dynamic imaging of the upper airway during tidal breathing," *Magn Reson Med*, 70(6): 1580-1590, 2013.
[10] Chu, WCW, Ng, BKW, Li, AM, Lam, T, Lam, WWM, Cheng, JCY.: "Dynamic magnetic resonance imaging in assessing lung function in adolescent idiopathic scoliosis: a pilot study of before and after posterior spinal fusion," *Journal of Orthopedic Surgery and Research*, 2-20: 1-7, 2007.
[11] Tong YB, Udupa JK, Ciesielski KC, Wu C, McDonough JM, Mong DA, Campbell RM, Jr. Retrospective 4D MR image construction from free-breathing slice Acquisitions: A novel graph-based approach. Med Image Anal. 2017;35:345-59.
[12] Zhuge Y, Udupa JK, Liu J, Saha PK. Image background inhomogeneity correction in MRI via intensity standardization. Comput Med Imaging Graph. 2009;33(1):7-16.
[13] Nyul LG, Udupa JK. On standardizing the MR image intensity scale. Magn Reson Med. 1999;42(6):1072-81.
[14] Tong YB, Udupa JK, Odhner D, Wu CY, McDonough JM, Capraro A, Torigian DA, Campbell RM. IRFC Interactive iterative relative fuzzy connectedness lung segmentation on thoracic 4D dynamic MR images, SPIE Medical Imaging 2017, 1013723-1013723-6, 2017.
[15] Mayer, O, Redding, G: "Early changes in pulmonary function after vertical expandable prosthetic titanium rib insertion in children with thoracic insufficiency syndrome," *Journal of Pediatric Orthopaedics*, 29(1):35-38, 2009.
[16] Zeger SL, Liang KY, Albert PS.: "Models for Longitudinal Data: A Generalized Estimating Equation Approach," Biometrics, Vol. 44(4): 1049-1060, 1988.
[17] Gollogly S, Smith JT, White SK, Firth S, White K.: "The volume of lung parenchyma as a function of age: A review of 1050 normal CT scans of the chest with three-dimensional volumetric reconstruction of the pulmonary system," *SPINE*, 29 (18): 2061-2066, 2004.